The effect of in-situ metasomatism on the electrical resistivity of the lower crust

S. Jennings [a,*], D. Hasterok [a], M. Hand [a], K. Bhowany [a,b]

[a] Department of Earth Sciences and Mawson Centre for Geoscience, University of Adelaide, Australia
[b] W.H.Bryan Mining & Geology Research Centre, Sustainable Minerals Institute, The University of Queensland, St Lucia Campus, QLD 4072, Australia

A R T I C L E   I N F O

A B S T R A C T

Improved estimates of composition and temperature in the lower crust are vital in characterising crustal rheology and better understanding tectonic processes. Fluids introduced into the lower crust during collisional events leave behind large domains of metasomatised crust which are long-lived and should be observable via magnetotelluric sounding. With this in mind, the electrical conductivity of a subduction-related eclogite and its anhydrous, anorthositic granulite protolith were experimentally determined at atmospheric pressure and lower crustal temperatures (773–1123 K). Complex impedance spectra were collected between 20 Hz and 2 MHz while oxygen fugacity was controlled about the quartz-fayalite-magnetite (QFM) buffer using a $CO:CO_2$ gas mix. At <1000 K, both samples are characterised by impurity conduction with low observed activation enthalpies of 0.48 ± 0.03 eV and 0.39 ± 0.02 eV for the granulite and eclogite respectively. High temperature data from the granulite (>1000 K) indicates a switch to small polarons with an activation enthalpy of 1.02 ± 0.02 eV. Results indicate that conversion of Fe-poor mafic granulite to eclogite does not enhance conductivity at lower crustal temperatures. Comparisons with previous experiments reveal a much stronger relationship between conductivity and FeO_T than previously anticipated. Modelling indicates that an increase in FeO_T of 2 wt% is equivalent to a temperature increase of 100 K and reasonable variations in FeO_T in the lower crust may account for $\sim$4 orders of magnitude variation in conductivity. Elevated FeO_T up to 20 wt% may enhance conductivity to $\sim 10^0$ S m^{-1} at a moderate 873 K. A system of linear equations is derived to estimate iron content, electrical conductivity or temperature within dry, mafic lower crust. For the temperature range 773–973 K, conductivity may be predicted to within 0.16 log units using $\log \sigma(T,FeO_T) = 0.006\,T + 0.3FeO_T - 11.35$. Under the same conditions, FeO_T may be predicted to within 0.51 wt% using $FeO_T(T,\sigma) = 37 - 0.0193\,T + 3.24 \log \sigma$. Finally, lower crustal temperatures may be estimated to within 24 K using $T(FeO_T,\sigma) = 1728 - 42FeO_T + 139 \log \sigma$.

1. Introduction

The emergence of magnetotelluric (MT) imaging as a means for resolving lithospheric scale features has led to a marked increase in its use across a multitude of research and industry applications. Over time, many MT studies have revealed the presence of large-scale, deep crustal conductors that largely belie our current understanding of the structure and composition of the lower continental crust (e.g. Shankland and Ander, 1983). Some discussion exists around whether such features are inherent to the lower crust or merely regional characteristics defined by both composition and tectonic setting (Yang, 2011; Selway, 2014, 2018); however, it remains that the cause of such features are still not well understood.

Simply defining the lower crust in terms of depth, composition and expected temperatures is a challenging task so it is no surprise that an all-encompassing explanation for electromagnetically-induced, lower crustal phenomena is not readily forthcoming. The depth of the lower crust is typically estimated using seismic wave speeds and most studies place the upper and lower bounds of such a layer somewhere between 20 and 40 km deep (Rudnick and Gao, 2014; Huang et al., 2013). Although variable from region to region, generally elevated wave speeds suggest a broadly mafic lower crust with analyses on xenolith and exposed lower crustal terranes indicating anhydrous mineral assemblages typical of granulite facies (Rudnick and Gao, 2014; Huang et al., 2013).

While the original use of the term granulite described a rock of granular texture and strong banding, the term now almost ubiquitously

---

identifies rocks of the granulite facies, a group of high-grade metamorphic rocks that have experienced conditions of at least 973 K and a minimum of 0.2 GPa (Wright, 1990). It is unclear whether xenoliths or granulite-facies terranes best represent the lower crust so there is some degree of uncertainty surrounding the appropriate use of one over the other (Hacker et al., 2015; Rudnick and Gao, 2014). Despite this, a number of laboratory experiments have been carried out to characterise the electrical conductivity of granulites under lower crustal conditions (Fuji-ta et al., 2004; Li et al., 2010; Bagdassarov et al., 2011; Sun et al., 2019).

Due to the complexity of measuring whole-rock samples, similar studies have focused on individual minerals measured at lower crustal conditions including plagioclase, clinopyroxene, orthopyroxene and garnet (e.g. Romano et al., 2006; Yoshino et al., 2008; Yang et al., 2011a, 2011b; Dai et al., 2012; Hu et al., 2013; Zhang and Yoshino, 2016). Detailed knowledge on the conductivity of individual minerals allows researchers to model conductivity of the entire crustal column using mixing relationships based on predicted mineral proportions (Selway, 2018; Ozaydın and Selway, 2020). Such modelling tends to neglect the effect on conductivity of compositional variations in solid-solution minerals, e.g., albite to anorthite, so applications to the lower crust are somewhat limited.

In tectonically active settings, fluids may be released into the lower crust in a number of ways, including through subduction-related dehydration reactions, and are shown to significantly enhance conductivity (e.g. Wannamaker et al., 2009). Under stable conditions, free-fluid in the lower crust is consumed by the host rock (Yardley and Valley, 1997), and often leaves behind metasomatic evidence in the form of in-situ eclogitisation although the exact product depends on the pressure and temperature conditions and the availability of fluid (Austrheim, 2013). Subduction-related eclogites have been shown to exist for billions of years provided subsequent thermotectonic events do not overprint or destroy the initial eclogite assemblages (Tamblyn et al., 2020). It therefore stands to reason that wide-spread eclogitisation of previously anhydrous granulite-facies rocks may be pervasive throughout the lower crust in the form of ancient subduction zones.

Rocks of the eclogite facies are defined by their conditions of formation in high to ultra-high pressure environments rather than a specific composition (Austrheim, 2013). As such, eclogites may encompass an extremely broad range of compositions entirely dependent on the protolith and chemistry of fluid catalysts. Electrical conductivity of eclogites have been characterised by a number of laboratory experiments (e. g. Laštovičková and Parchomenko, 1976; Bagdassarov et al., 2011; Guo et al., 2014; Dai et al., 2016) as well as their common constituent minerals such as garnet and omphacite (Liu et al., 2019). Earlier results from Laštovičková and Parchomenko (1976) found their eclogite samples from the Bohemian Massif in Central Europe to be largely variable in conductivity, ranging anywhere from 10^{-4} to 10^{-2} S m^{-1} between ~773–973 K. While their DC and single frequency AC experimental techniques are now outdated, more modern approaches to electrical conductivity measurements are in general agreement with their findings (Bagdassarov et al., 2011; Guo et al., 2014; Dai et al., 2016). Of course, direct comparisons between otherwise unrelated studies are not always suitable as doing so disregards variation in composition between the different samples.

At temperatures representative of the lower crust, silicate minerals and rocks behave as semi-conductors and conductivity is governed by diffusion of charged particles such as hydrogen, cation species such as K$^+$ and Na$^+$, and "hopping" of electron holes (small polarons) between ferric (Fe^{3+}) and ferrous (Fe^{2+}) iron (Chakraborty, 2008). As such, besides temperature, bulk composition is possibly the largest contributor to variations in electrical conductivity between single rock types (Dai et al., 2016). Therefore, to truly understand the effect on conductivity due to the eclogitisation of lower crustal granulite, it is imperative that direct comparisons are made only between an eclogite and its direct protolith. Such regions are rare at the surface but certainly exist.

The Bergen Arcs in Norway record ancient fluid interaction with predominantly anhydrous granulite in the lower crust that lead to wide-scale eclogitisation. Now exposed at the surface, the relationship between altered rock and granulite protolith is expressed on the metre to decimetre scale in the form of widespread, fluidic shear zones. In addition, the fluid catalyst has been shown to not significantly alter chemistry such that both samples reflect a broadly similar anorthositic bulk composition (Austrheim, 2013). The area therefore represents a fine opportunity to study the direct effect of fluid alteration within a granulite-facies terrane of lower crustal origin.

In this study, we determine the electrical conductivity of an eclogite and its immediate granulite protolith at simulated temperature conditions analogous to the lower crust. Oxygen fugacity (fO$_2$) is controlled between the quartz-fayalite-magnetite (QFM) buffer and QFM + 2 log units in order to quantify the effect of fO$_2$ on the conductivity of lower crustal rocks. We compare results from both samples to comment on the electrical properties of eclogitised crust and the potential for using crustal-scale resistivity models to image ancient subduction zones. A brief analysis of our results in comparison to previous experiments on both rocks and minerals highlights the dominant conduction mechanisms in both samples. Finally, we develop predictive models that allow us to estimate properties of the lower crust including electrical conductivity, FeO$_T$ and temperature. In complement to modern seismic investigations, these models have the ability to provide further insight into the composition and rheologic nature of the lower crust using magnetotelluric methods.

2. Sample characterization and preparation

The samples used in this study were collected from the Island of Holsnøy in south-western, Norway as part of previous projects undertaken by the University of Adelaide (Fig. 1a). The geology of Holsnøy makes up part of the Lindås Nappe, one of the predominant arcuate, Caledonian thrust sheets defining the Bergen Arcs (Austrheim, 2013). The region is special in that it superbly records the interaction of ancient fluids with nominally anhydrous, Neoproterozoic anorthositic granulite leading to widescale eclogitisation (Bhowany et al., 2017).

Details of the fluid-catalysed conversion process, associated with subduction of continental crust during the Caledonian Orogeny (c. 450 Ma), have been documented extensively by numerous studies (e.g. Austrheim, 2013; Bhowany et al., 2017). The granulite-facies terrane predominantly consists of rocks composed of plagioclase with lesser amounts of clinopyroxene, orthopyroxene and garnet with peak metamorphic conditions estimated at 1 GPa and 1073 to 1173 K (Austrheim, 2013). Peak mineral assemblage of the eclogite consists of zoisite, phengite, omphacite and garnet with phase equilibria forward modelling determining peak metamorphic conditions of ~2.1–2.22 GPa and 943–963 K (Bhowany et al., 2017). Hydrous phases in the eclogite, such as phengite and zoisite, indicate the presence of fluid during formation (Austrheim, 2013) and detailed analysis of fluid inclusions suggest a mixture of N$_2$ with CO$_2$ and/or H$_2$O (Andersen et al., 1993). Eclogites in the region occur as shear zones of variable thickness (Fig. 1b, c and d) and represent pathways of fluid flow through the granulite protolith (Austrheim, 2013). The samples used in this study were separated by a distance of ~1 m and were taken from either side of a distinct fluid-alteration interface.

Whole-rock geochemistry was performed on fused disks prepared using a lithium tetraborate flux and determined using wavelength dispersive X-ray fluorescence (WD–XRF) spectrometry at the Department of Earth and Environment, Franklin and Marshall College, Lancaster PA. Results from the analysis can be found in Table 1 alongside an estimated bulk composition of the lower crust (Rudnick and Gao, 2014) and calculated compositions of both granulite and eclogite using the global geochemical database of Gard et al. (2019). Both samples are typical of the region but atypical in terms of global averages with regards to both Al$_2$O$_3$ and Fe$_2$O$_3$. Al$_2$O$_3$ is much higher in both samples,
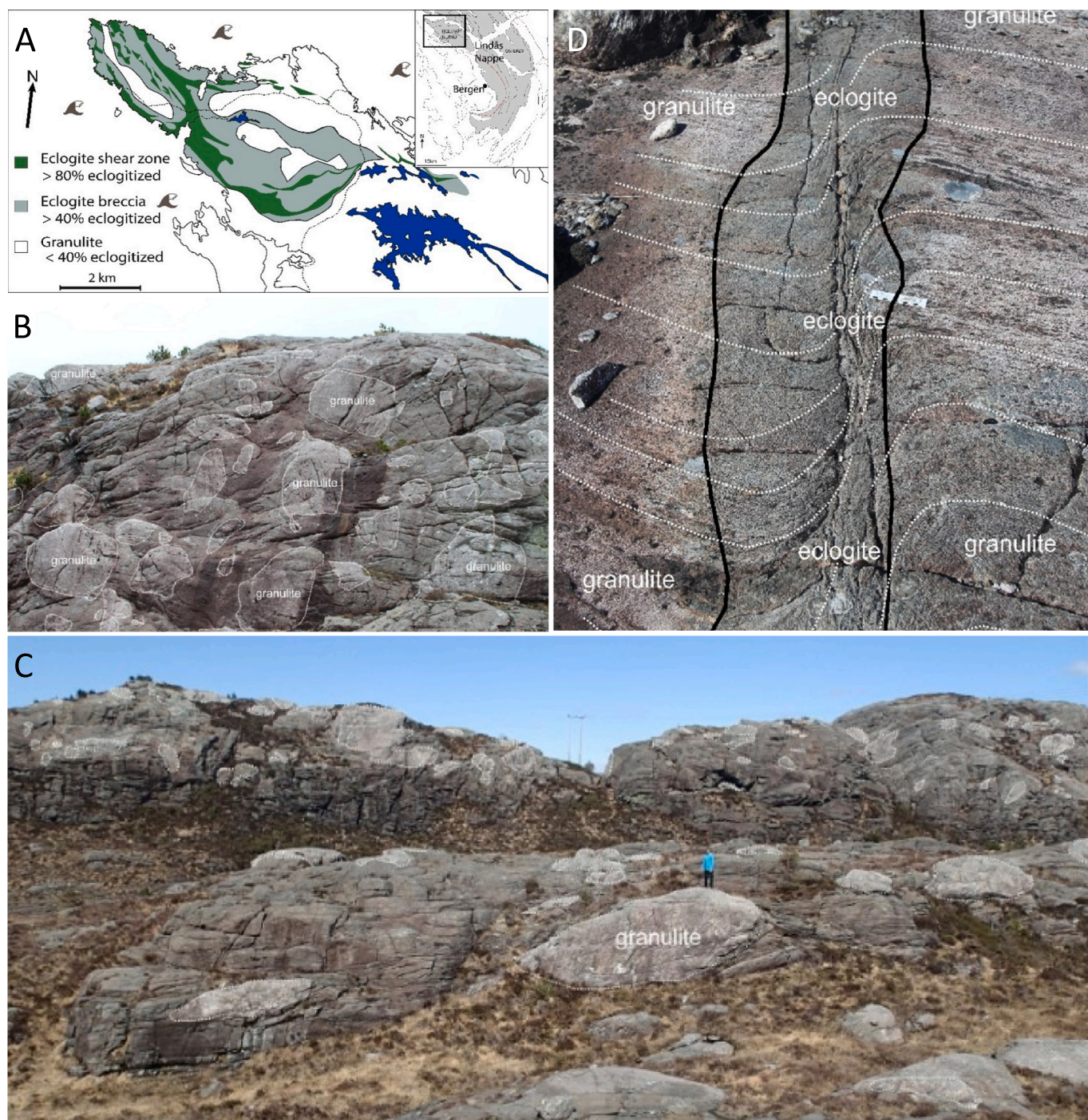
Fig. 1. a) Location of Holsnøy in SW Norway (inset), showing the regional pattern of fluid-driven conversion of granulite to produce eclogite (adapted from Austrheim (2013)). b–d) Scales of granulite to eclogite transition. b) Small scale shear zone with localised reaction. c) Blocks of granulite (outlined) within eclogite. d) Large-scale conversion to eclogite. Isolated blocks of residual granulite (outlined) within a km-scale eclogite shear zone.

by ~10 wt%, compared to global averages while Fe₂O₃ is only half as much.

Modal mineralogy was determined as part of this thesis using the scanning electron microscope (SEM) at Adelaide Microscopy, University of Adelaide, South Australia. The granulite sample is typical of the region, consisting predominantly of plagioclase (62%), garnet (27%) and lesser clinopyroxene and K-feldspar (6% and 3%). Plagioclase defines the bulk of the matrix, with grains ranging 0.5–1 mm, and is often surrounded by a thin veneer of K-feldspar (Fig. 2). Garnet crystals range in size from 0.5 to 2 mm and are often interconnected, but not to such a degree where they span the thickness of the sample. Grains of

clinopyroxene, approximately 0.5 mm, occur throughout and almost always occur in direct contact with garnet. The eclogite is also typical of the region and consists of mostly omphacite (40%) alongside garnet (25%), zoisite (15%) and kyanite (13%), as well as minor phengite and albite. Omphacite, zoisite and kyanite make up the fabric of the sample with scattered garnet, 0.5 to 1.5 mm, occurring throughout. Phengite, ~3%, occurs sporadically throughout the sample while relict plagioclase, ~1%, indicates that insufficient fluid was present in this particular sample to achieve full eclogitisation.

Hand sample size specimens of both rock types were initially cut into slabs approximately 5 mm thick. A number of representative areas were

Table 1

Whole-rock geochemistry for our granulite and eclogite samples presented alongside an estimate of the bulk lower crust (Rudnick and Gao, 2014) and computed statistics from the Global Geochemical Database (Gard et al., 2019). All FeO and Fe₂O₃ converted to total iron (FeO$_T$).

wt%	L.Crust	Granulite				Eclogite			
		This Study	μa	σ	$\pm$	This Study	μb	σ	$\pm$
SiO$_2$	53.4	51.22	57.46	9.84	−6.24	45.37	49.08	3.93	−3.71
TiO$_2$	0.82	0.11	0.85	0.52	−0.74	0.18	1.17	0.76	−0.99
Al2O3	16.9	26.18	15.63	2.60	10.55	27.34	15.81	2.74	11.53
FeO$_T$	8.57	4.04	8.24	4.23	−4.20	3.18	10.44	4.06	−7.26
MnO	0.1	0.07	0.14	0.08	−0.07	0.09	0.18	0.07	−0.09
MgO	7.24	4.11	5.31	4.06	−1.20	5.52	8.40	4.05	−2.88
CaO	9.59	9.13	7.17	4.24	1.96	12.16	10.48	2.82	1.69
Na$_2$O	2.65	4.18	2.73	1.27	1.45	2.97	2.74	1.37	0.23
K$_2$O	0.61	0.5	1.33	1.24	−0.83	0.22	0.46	0.44	−0.24
P2O5	0.1	0.03	0.16	0.13	−0.13	0.03	0.13	0.11	−0.10
Total		100.02				99.93			
LOI		0.7	0.57	0.54	0.13	1.14	0.90	0.72	0.24

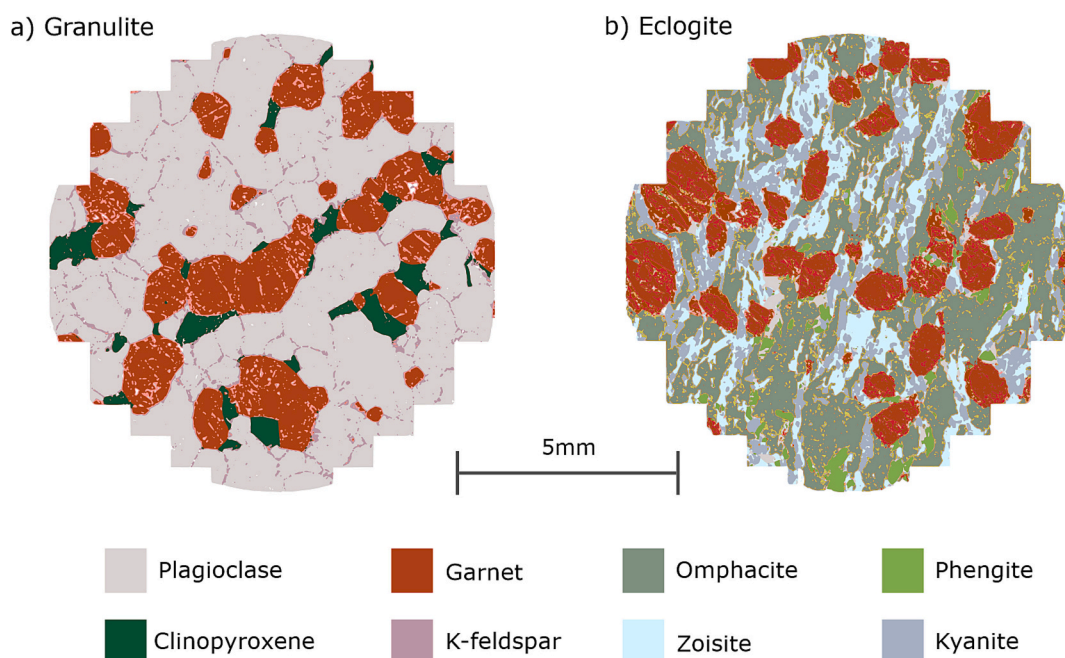a) $n = 4260$; b) $n = 1068$; LOI = loss on ignition

Fig. 2. Output from the Scanning Electron Microscope at Adelaide Microscopy used to determine modal mineralogy for both samples. a) Granulite – 62% plagioclase, 27% garnet, 6% clinopyroxene and 3% K-feldspar. b) Eclogite – 40% omphacite, 25% garnet, 15% zoisite, 13% kyanite, 3% phengite.

identified and sampled in both specimens using a 12 mm diameter, diamond tipped, coring drill bit. A single disc from each was then selected for the experiment and both sides ground flat until parallel. Both samples were mounted in an epoxy resin casing with a single surface exposed and polished before sending to Adelaide Microscopy for analysis using the SEM. Standard procedures for the SEM dictate that a thin carbon film is applied to the exposed surface which required removal on completion. Post analysis, the sample was fully submerged in ethanol for 24 h in an attempt to soften the epoxy resin before prying the sample free. Finally, both sides of each sample were ground down again to ensure no trace of resin or carbon on any surface. The final samples used in the experiment were approximately 4–4.5 mm thick with a radius of 5.5 mm.

3. Setup and experimental methods

Complex impedance spectra were collected over the frequency range 20 Hz to 2 MHz at regular intervals using a two-electrode, spring loaded cylinder apparatus connected to a Keysight E4980A/AL Precision LCR Meter (Fig. 3). The measurement cell sits within a highly-resistive,

alumina cylinder which is threaded through a custom-built tube furnace capable of reaching temperatures up to 1473 K, although the open nature of our setup limits experiments to a practical maximum of ~1373 K. Inside the measurement cell, iridium foil is placed between the Pt–Pt$_{90}$Rh$_{10}$ (S-type) thermocouples and the sample in order to prevent Fe-loss to the electrodes. The electrodes themselves are 10 mm in diameter and large enough to cover almost the entire face of each sample. Temperature data were collected using the internal multimeter of a Keysight E34972A LXI Data Acquisition Unit (DAQ) and are reportedly accurate to 0.6–1.5 K over the experimental temperature range.

Our study involved two separate experiments that ran for approximately 2.5 weeks each and were fully automated using a custom scripted program. Both experiments were conducted at standard atmospheric pressure and cover the same fO$_2$ range, spanning from the QFM buffer to an upper limit of QFM + 2 log units. Oxygen fugacity of the lower crust is likely to be somewhere between the QFM and Ni-NiO buffer (Bose et al., 2009; Harlov, 2000; McCammon, 2005). We control fO$_2$ throughout the experiment using a CO$_2$:CO gas mix passed into the apparatus and across the sample using three Alicat Mass Flow Controllers; one controlling the
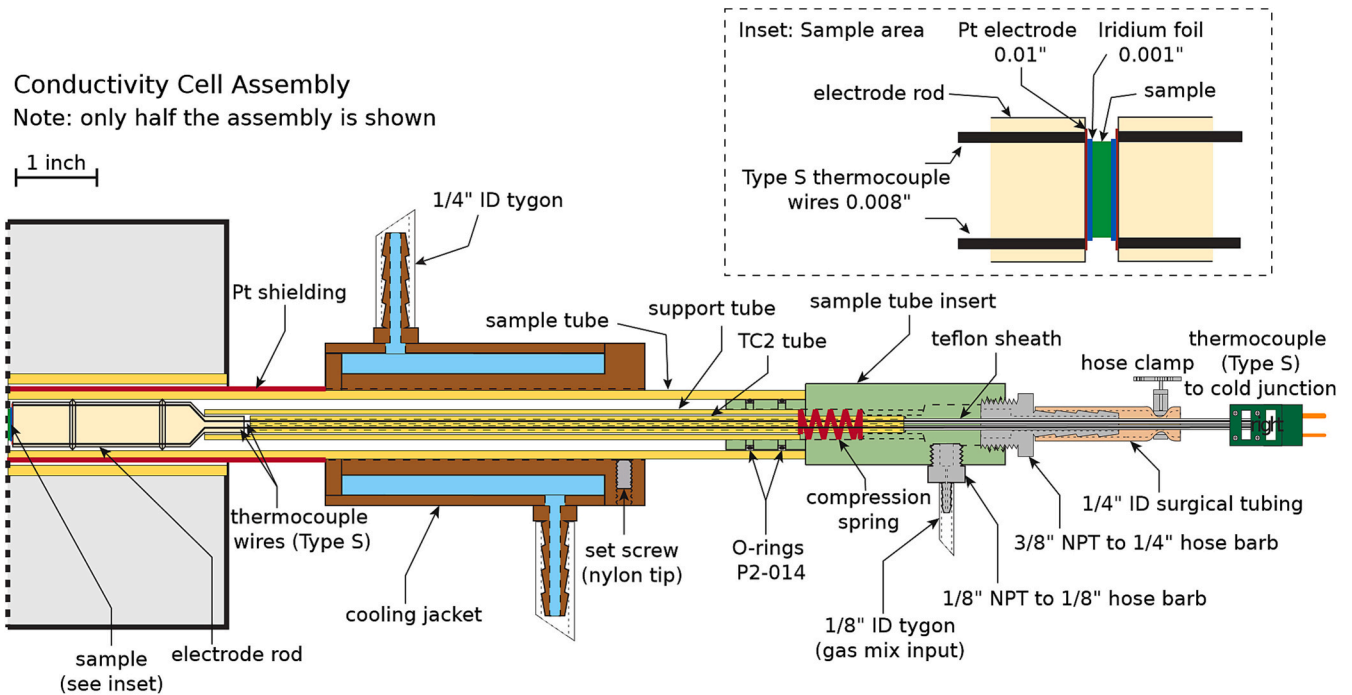
Fig. 3. Schematic of the electrical conductivity cell assembly in use at the University of Adelaide.

flow of CO_2 and two controlling CO. While pressure has been shown to have minimal effect on electrical conductivity (e.g. Guo et al., 2014; Sun et al., 2019; Zhang and Yoshino, 2016), the effect of microcracks on samples measured at atmospheric pressure could potentially influence our results (Dai et al., 2016). We attempt to mitigate this by sourcing samples from recently exhumed materials and selectively sampling from parts of the rock that are visually absent of fractures, weathering and alteration.

The granulite experiment involved five separate temperature runs from 873 to 1023 K, with each run increasing fO_2 by 0.5 log units. Measurements were taken during both heating and cooling cycles in order to assess the sample for potential Fe-loss or significant alteration throughout the experiment. Upon initial heating, the sample was left to equilibrate to the desired fO_2 at 873 K for 48 h and each subsequent gas change was allowed a further 36 h for re-equilibration. Uncertainty in the melting point of the eclogite and experience gained from the previous experiment saw us change the experimental procedure slightly for the eclogite sample. The experimental temperature range was reduced to between 773 and 973 K and only three temperature runs were conducted using fO_2 step changes of 1 log unit. The initial equilibration period was also increased to a full week and the inter-run re-equilibration periods were doubled to 72 h.

The reduced temperature range for the eclogite experiment was a precautionary measure to prevent unintentional melting of the sample. Such an event would require cessation of the experiment, render the sample unsuitable for further analysis and has potential to seriously damage equipment. The melting point of the sample was estimated roughly at between 1023 and 1073 K based on previous PT modelling undertaken on similar samples while also accounting for ambient pressure conditions. The final experimental upper limit of 973 K was selected to provide a 50 K buffer around these estimates.

4. Results

Representative impedance spectra for both samples controlled at the QFM buffer are illustrated in Fig. 4. Both show the onset of a semicircular arc at lower frequencies consistent with observations in similar experiments interpreted to represent the bulk impedance of the

rock. Many experiments measure impedance at frequencies as low as 0.1 Hz which allows them to fully characterise this low frequency arc as well as contact effects between the sample and electrodes, however, our high sample resistance and minimum frequency limit of 20 Hz means we fail to do the same. In fact, significant noise in our low frequency data forced us to reject any data below 200 Hz during modelling which further restricted our impedance modelling of the larger arc.

A secondary arc of much smaller magnitude is observed at higher frequencies (> 12 KHz) and simultaneously modelled with the larger arc using an equivalent circuit model consisting of two resistor-capacitor (RC) pairs connected in series. Multiple arcs can be a sign of conduction both through grain interiors and along grain boundaries (Tyburczy and Roberts, 1990); however, separate modelling of both arcs reveals that the high frequency arc has almost no temperature dependence. A lack of even moderate temperature dependence is unrealistic for diffusion in a semi-conductor so we exclude the high frequency arc when calculating conductivity of the sample and note that doing so serves to increase conductivity by ~0.1 log units across the lower experimental temperature range. We interpret that the high frequency arc is probably related to the experimental setup in some way but remains undiagnosed.

From this fit, we determine the sample resistance of both the eclogite and granulite across a wide range of temperatures akin to the lower crust using

$$\sigma = \frac{L}{AR}, \tag{1}$$

where conductivity, σ, the sample thickness, L, the cross-sectional area of the electrode covered faces, A, the sample resistance, R.

Across comparable temperatures, both the granulite and eclogite are extremely resistive (Fig. 5).

Over the entire experimental temperature range of 873 to 1023 K, the granulite sample increases by approximately one order of magnitude from $10^{-5.1}$ to $10^{4.1}$ S m^{-1}. The eclogite sample was limited to a more confined temperature range of 773 to 973 K and increases in conductivity by around 0.3 log units during each temperature cycle. We encountered some issues modelling the eclogite conductivity at temperatures <843 K thanks to the high sample resistance at low temperatures. Under these conditions, our data fails to properly characterise
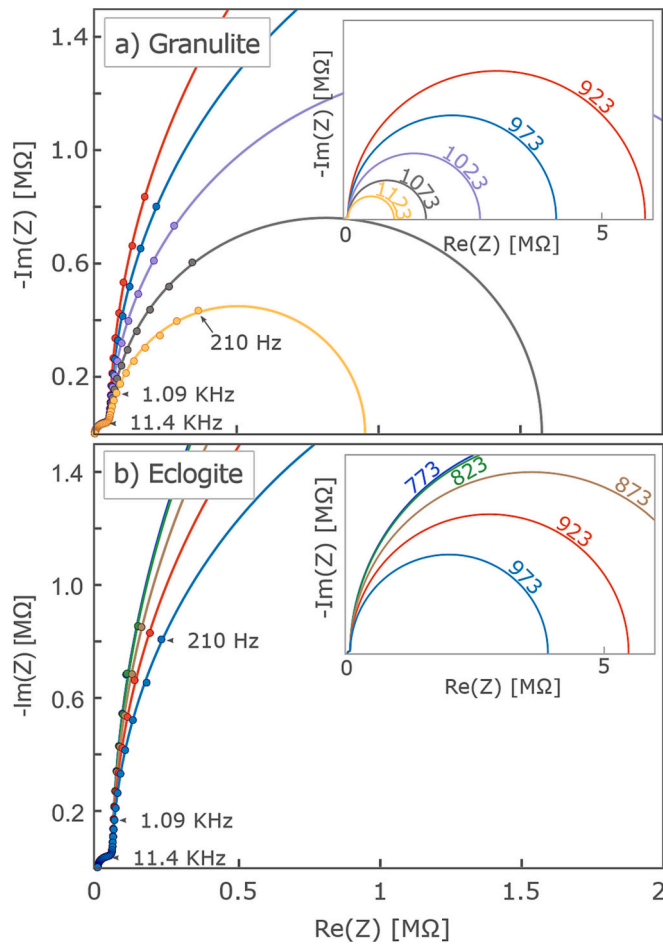
Fig. 4. Representative impedance spectra for the granulite from 923 to 1023 K and the eclogite from 773 to 973 K. Sample conductivity is calculated by fitting the impedance spectra to an equivalent circuit model consisting of two resistor-capacitor pairs connected in series. Insets provided to highlight the overall trend and magnitude of the fitted models. Note that despite being measured as part of the experiment, frequencies below 200 Hz are not displayed due to noise reulting from our experimental setup which, if displayed here, would significantly detract from the interpratability of the figure.

the impedance arc and our models begin to converge towards the same value. For this reason, the effective temperature range of our determined eclogite conductivities are 843 to 973 K.

Reproducibility between heating and cooling cycles during a temperature run is generally an indication that no in-situ metamorphism has occurred during our experimentation, nor has any Fe-loss to the electrodes taken place. While most of our data are reproducible, some of the earlier measurements, in particular during run 1 of the granulite sample, show a slight discrepancy between heating and cooling cycles. We do not believe this to be the result of alteration or Fe-loss (thanks to the use of iridium foil between the electrode and sample), but rather evidence that the sample was not yet at equilibrium with the new gas mix. Because of this, we choose to model data from granulite experiment using only the cooling cycles. The issue was fixed for the eclogite experiment by greatly increasing the time allowed for equilibration on initial heating and increasing the duration of re-equilibration steps after further changes to the gas mix. Reproducibility between heating and cooling runs also indicates that no dehydration reactions have occurred within hydrous minerals that make up most of the eclogite sample.

Silicate minerals and rocks behave as semi-conductors at temperatures characteristic of the lower crust. Charge carriers in a semiconductor are diffusing particles which will obey the Arrhenius relation
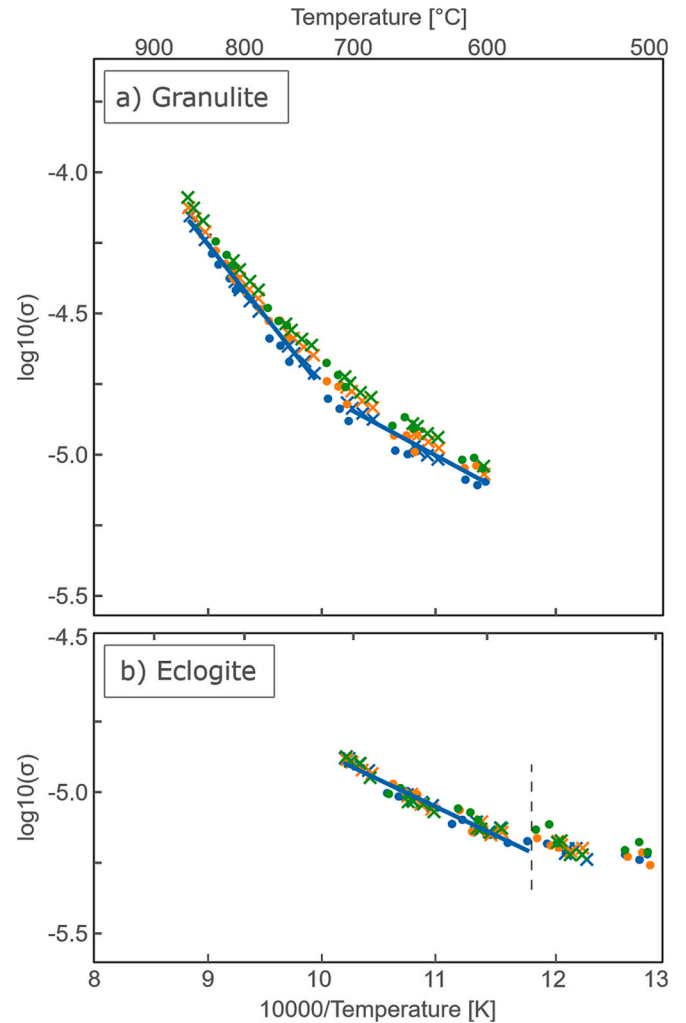
Fig. 5. Logarithm of electrical conductivity vs reciprocal temperature for both the granulite and eclogite at QFM (blue), QFM + 1 log unit (orange) and QFM + 2 log units (green). a) Granulite - Two lines are fit to the granulite data indicating two distinct conductive mechanisms. Only data from the cooling cycle are used due to slight hysteresis resulting from inadequate gas equilibration on the heating run. b) Eclogite - a single line is fit to data from the eclogite sample. Data below 843 K are rejected from modelling due to systemic limitations of the data below this point (see text for discussion). (For interpretation of the references to colour in this figure legend, the reader is referred to the web version of this article.)

$$\sigma = \sigma_0 \, exp \left(\frac{-\Delta H}{kT} \right), \tag{2}$$

where σ_0 is a pre-exponential factor, ΔH, the activation enthalpy of the diffusing species, k, the Boltzmann constant and T, the temperature in degrees kelvin. The equation above will produce a straight line on an Arrhenius plot (log σ vs inverse temperature) for a single conduction mechanism, from which the ΔH can be determined from the slope of the line. If more than one conduction mechanism is present, the observed result will be the cumulative effect of both mechanisms.

Using ordinary least squares regression, we are able to fit two distinct lines to our granulite data and a single line to our eclogite data (Fig. 5). Fit results and parameters are all recorded in Table 2. The slope of the high temperature granulite data equates to a ΔH of 1.02 eV ($r^2 = 0.995$) while the lower temperature data fits a much lesser slope equivalent to 0.48 eV ($r^2 = 0.968$). The change in slope occurs at approximately 1000 K signifying a change in the dominant conduction mechanism for the granulite sample at this temperature. Due to the restricted temperature

Table 2
Fitted parameters of the Arrhenius relationship for our lower crustal granulite and eclogite samples.

	T [K]	$\log_{10}(\sigma)$	ΔH [eV]	r2
Eclogite	843–973	−2.89 ± 0.105	0.39 ± 0.02	0.957
Granulite	873–1000	2.60 ± 0.18	0.48 ± 0.03	0.968
Granulite	1000–1133	0.36 ± 0.11	1.02 ± 0.02	0.995

range of our eclogite experiment only a low temperature slope was observed in our data from which we determine a ΔH of 0.39 eV, which is roughly equivalent to the low temperature ΔH of the granulite. The fit to the eclogite data ($r^2 = 0.957$) was slightly worse than the granulite due to increased noise at lower temperatures.

Variations in fO_2 were expected to be a large part of our experiment but we find only a limited effect on electrical conductivity for our granulite sample and no effect for the eclogite (Fig. 6). For the granulite sample, a small but clear increase in conductivity is evident with increasingly oxidised conditions, although the effect might be so small as to be considered negligible. At lower temperatures, data are slightly contaminated by noise due to uncertainty in the conductivity values as well as limitations in handling sensitive gas flows at very high CO_2:CO gas mix ratios. For the eclogite sample, no obvious trend is apparent with fO_2 at any temperature. Due to the limited effect of fO_2 on our results, we only model the available data measured at the QFM buffer.

5. Discussion

In laboratory studies such as this one, it is essential to first determine the dominant conduction mechanism for each sample. Conduction mechanisms in silicate rocks are often determined from activation enthalpy, ΔH, and knowledge of the potential charge carriers. As a general rule, under lower crustal conditions a small ΔH is characteristic of proton (or impurity) conduction, moderate values relate to small polaron hopping and larger values are indicative of ionic conduction (Selway, 2014). With regards to Eq. 2, each of these mechanisms will
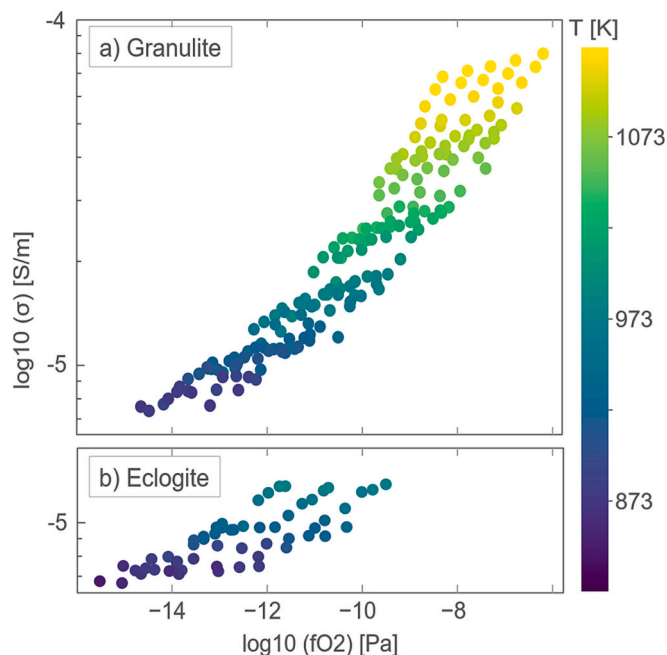

Fig. 6. Logarithm of conductivity versus the logarithm of oxygen fugacity. a) Granulite – a small but clear trend is evident between conductivity and oxygen fugacity for the granulite sample. b) Eclogite – no apparent trend is evident between conductivity and fugacity over the limited temperature range of the eclogite experiment.

dominate over a particular temperature range with ionic conduction reserved for the highest temperatures and unlikely to greatly affect conductivity under typical lower crustal conditions. The distinction between mechanisms is not always clear, so comparison with previous experiments on similar lower crustal rocks and minerals is often necessary. When the dominant mechanisms are identified, it is then possible to address wider implications such as the effect of composition and eclogitisation on bulk conductivity.

5.1. Conduction mechanisms

At low temperatures, slope and magnitude are roughly equivalent for both samples (Table 2; Fig. 5), therefore it is likely the conductive mechanism below ~1000 K is the same in each. The observed ΔH of 0.38 and 0.43 eV for our eclogite and granulite are consistent with low temperature data from previous experiments for a range of crystalline rock types (Table 3). Most studies indicate that ΔH in the range 0.36–0.5 eV can be attributed to impurity conduction at low temperatures (Sun et al., 2019; Dai et al., 2014; Bai et al., 2002).

Above ~1000 K, ΔH increases to 1.02 eV, indicating a change in the dominant conduction mechanism. Our granulite consists predominantly of plagioclase, garnet and clinopyroxene (Fig. 2); therefore, results from past experiments on these minerals may hint towards the dominant mechanism in our own sample (Fig. 7. Plagioclase in our granulite is near identical in composition to that measured by Yang et al. (2011a, $An_{55}Ab_{45}$) who determined a ΔH of 1.67 eV which they attribute to diffusing Na^+ ions. As our sample exhibits a far smaller ΔH, we expect that Na^+ diffusion in plagioclase is likely not the dominant mechanism. A more recent systemic study on electrical conductivity of plagioclase has shown ΔH values ranging from 0.71 to 1.09 eV (Hu et al., 2022). Given the relatively high modal abundance of plagioclase in our granulite, it is possible that conduction through plagioclase is an important contributor to bulk conductivity.

Likewise, the garnet in our granulite ($Py_{38}Alm_{46}Grs_{15}$) is within the compositional range of natural samples measured by Dai et al. (2012) who attribute ΔH values ranging between 1.32 and 1.37 eV to small polaron diffusion. This is slightly higher than our measured ΔH of 1.02 eV but not unreasonable. Small polaron diffusion has also been shown to dominate conduction in Fe-bearing clinopyroxene (~$En_{40}Wo_{48}Fs_{12}$) with ΔH modelled at 1.06 eV (Yang et al., 2011b). This result is similar to our measured ΔH of 1.02 eV and the minor difference is easily

Table 3
Activation enthalpies and conduction mechanisms for previous experiments on lower crustal rock types. While the temptation is to group this table by rock type, we instead order by increasing ΔH to show that rock type is largely independent of the inferred conduction mechanism. Imp = impurity conduction. Ba02 (Bai et al., 2002), Fu04 (Fuji-ta et al., 2004), Li10 (Li et al., 2010), Ba11 (Bagdassarov et al., 2011), Da14 (Dai et al., 2014), Gu14 (Guo et al., 2014), Da16 (Dai et al., 2016), Da18 (Dai et al., 2018), Su19 (Sun et al., 2019).

Rock Type	Pressure	T (K)	ΔH (eV)	Mechanism	Reference
Granulite		570–870	0.35[†]	Imp[*]	Fu04
Granulite	1–3	623–723	0.36–0.42	Imp	Su19
Eclogite		843–973	0.39	Imp	This Study
Anorthosite	1	683–1023	0.42[†]	Imp	Ba02
Granite	0.5	623–773	0.44–0.5	Imp	Da14
Eclogite	2.5	500–650	0.45	Fe (H^+*)	Gu14
Granulite		873–1000	0.48	Imp	This Study
Granulite	1–3	623–1073	0.55–0.68	Fe	Su19
Granulite	1	523–1123	0.6	Fe*	Li10
Eclogite	2.5	646–1142	0.81[†]	H_2O (Fe*)	Ba11
Eclogite	1	873–1173	0.84	Fe	Da16
Granite	0.5	673–1173	0.93–1.18	K^+, Na^+	Da14
Eclogite	2.5	665–774	0.99	H^+ (Fe*)	Gu14
Granulite	1	681–1031	0.96–1.00[†]	Fe*	Ba11
Granulite		1000–1133	1.02	Fe	This Study

[†] remodelled from presented data.
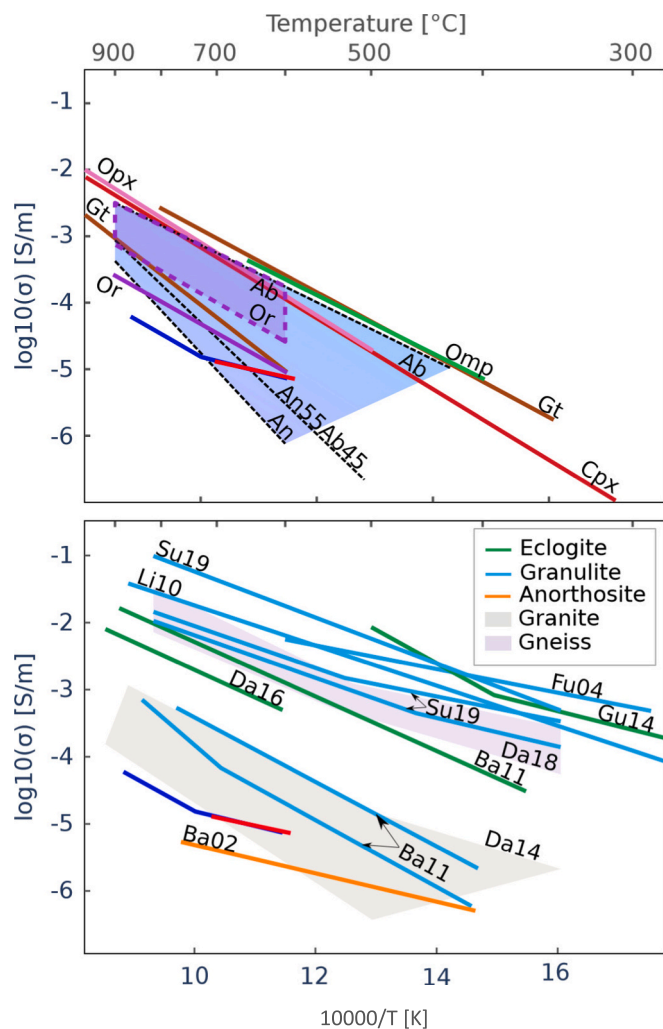[*] inferred conduction mechanism. See Section 5.2 for reasoning.

Fig. 7. Results from our granulite (dark blue) and eclogite (red) plotted against previous experiments on common lower crustal minerals (top) and potential lower crustal rock types (bottom). Mineral data sourced from the following: Plag (Yang et al., 2011a; Hu et al., 2013, 2015; Guo et al., 2015), Or (Hu et al., 2013, 2014), Gt (Dai et al., 2012; Liu et al., 2019), Opx (Yang et al., 2011a), Cpx (Yang et al., 2011b). Omp (Liu et al., 2019). Whole rock experimental data from the following: Ba02 (Bai et al., 2002), Fu04 (Fuji-ta et al., 2004), Li10 (Li et al., 2010), Ba11 (Bagdassarov et al., 2011), Da14 (Dai et al., 2014), Gu14 (Guo et al., 2014), Da16 (Dai et al., 2016), Da18 (Dai et al., 2018), Su19 (Sun et al., 2019). (For interpretation of the references to colour in this figure legend, the reader is referred to the web version of this article.)

explained by compositional variations, i.e. different Fe_{total} or Fe^{3+}, or variations in the connectivity and clustering of Fe^{3+} to Fe^{2+} (Yang et al., 2011b).

Another indicator that conduction in our granulite is likely driven by small polarons is that increased fO_2 has a positive effect on conductivity (Fig. 6). This effect is attributed to increased Fe^{3+} relative to Fe^{2+} resulting from increasingly oxidised conditions in Fe-bearing samples (Dai et al., 2012). Therefore, given the similar results between our granulite experiment and those on garnet and clinopyroxene, as well as the positive relationship between conductivity and fO_2, we believe our high temperature data represents small polaron conduction through both garnet and clinopyroxene.

5.2. Comparison with previous experiments

5.2.1. On granulites
Fuji-ta et al. (2004) measured the conductivity of a sintered granulite

sample over the temperature range 570 to 870 K and observe high conductivity at relatively low temperatures. It is possible that inadvertent oxidation of Fe ions during the sintering process may have led to their high observed conductivity; however, they report no detectable change in Fe ions in their sample. Unfortunately, they do not provide model parameters or suggest a conduction mechanism so we instead re-model their plotted data to obtain a ΔH of 0.35 eV. This particularly low ΔH may indicate that impurity conduction is the dominant mechanisms and Fe has little effect on their observed conductivity.

Li et al. (2010) measured a two-pyroxene granulite and observe high conductivities comparable to Fuji-ta et al. (2004); however, their modelled ΔH of 0.6 eV is almost double that of the former experiment. Li et al. (2010) also do not indicate a conduction mechanism but we infer it to be small polarons based on similarity to other experiments on granulites (Sun et al., 2019) (see Table 3). This inference is slightly at odds with our own results where we attribute a ΔH of 1.02 eV to small polarons, though differences are possibly explained by variable measurement conditions, i.e. different pressures, and vastly different.

FeO_T concentrations (12.85 wt% compared to our 4.04 wt%).

Activation enthalpies from Sun et al. (2019) are also much smaller than our granulite; however, their reported mineralogy is markedly different to ours and probably more indicative of middle crust (28–45% quartz, 13–30% biotite, 30–50% plag). Their conclusions that small polarons in biotite are responsible for ΔH in the range 0.55–0.68 eV is based on comparisons with hydrous, Fe-bearing minerals such as amphibole (0.64–0.81 eV) and chlorite (0.56 eV) and rocks such as phyllite (0.64–0.81 eV) (Wang et al., 2012; Manthilake et al., 2016; Sun et al., 2017). Our granulite is composed of nominally anhydrous minerals which may explain the difference in ΔH values despite the same reported conduction mechanism.

Bagdassarov et al. (2011) measure two granulites and an eclogite, finding the eclogite to be approximately one order of magnitude more conductive than the granulites at lower crustal conditions. They do not specify a conduction mechanism for their granulite samples but observed ΔH values of 0.96 and 1.0 eV for granulite below ~1000 K. These values are similar to our high temperature granulite data so we suggest that their results at the specified temperature range are possibly indicative of small polarons. Compared to previously mentioned granulite results, the Bagdassarov et al. (2011) samples are significantly less conductive, a fact they attribute to minor differences in individual mineral compositions. Despite this, their samples are still an order of magnitude more conductive than our own, a discrepancy we attribute to bulk Fe-content.

5.2.2. On eclogites
Carrying on from the previous section, while the eclogite measured by Bagdassarov et al. (2011) may exhibit high conductivity compared to their own granulite samples, it is less conductive than many granulites from other experiments (Fuji-ta et al., 2004; Li et al., 2010; Sun et al., 2019). This appears to indicate that eclogite mineral assemblages will not necessarily lead to enhanced conductivity in the lower crust. Compared to earlier work on eclogites (Laštovičková and Parchomenko, 1976), Bagdassarov et al. (2011) suggest their slightly higher conductivity and ΔH (0.81 eV) is due to high proportions of omphacite to garnet as water is preferentially partitioned into the former (Katayama et al., 2006). While this explanation is not unreasonable, they arrived at this conclusion by comparing their results against a previous experiment (Laštovičková and Parchomenko, 1976) which appears to be plotted in an incorrect position. In addition, their ΔH and bulk conductivity values are more comparable with later experiments that instead attribute conductivity to small polarons (Dai et al., 2016). Their conclusions also cannot explain why our eclogite remains incredibly resistive despite a large fraction of 40% omphacite and only 25% garnet. Of course, we do not measure water content in our sample so this last point is speculative.

Laštovičková and Parchomenko (1976) were among the first to measure conductivity of eclogites but their results are hard to reconcile

given the large range of reported values for a single rock type. This large range conductivities are attributed to variable symplectite content; however, their DC and single-frequency.

AC techniques have more recently been demonstrated to cause systematic errors (Karato and Dai, 2009) which may have affected their results. In addition, their experiments pre-date the use of gas mixtures that control the oxidation state of samples during high temperature experimentation. Depending on Fe content, failing to account for this has the potential to drastically affect their results and, unfortunately, they provide no geochemistry. A brief examination of other eclogites from the same region suggest Fe_2O_3 content is potentially highly variable between 6.13 and 16.09 wt% (Medaris et al., 1995).

Guo et al. (2014) observe high conductivity at low temperature for their lower crustal eclogite and attribute this to compositional differences between their sample and previous experiments (e.g. Laštovičková and Parchomenko, 1976; Bagdassarov et al., 2011). Their derived ΔH of 0.45 eV for $T < 650$ and 0.99 eV for $T > 665$ are in good agreement with our own, although the change in mechanism occurs at a much lower temperature. Guo et al. (2014) suggest hydrogen (impurity) conduction at high temperatures and small polaron conduction at low temperature which is at odds with the general sentiment for conduction in silicates (Selway, 2014). Given the similarity of their reported ΔH values with multiple experiments that conclude the exact opposite (Table 3), we suggest that the eclogite sample of Guo et al. (2014) is perhaps instead driven by small polarons at high temperature and impurity conduction at low temperature. We also note that their eclogite has abnormally high FeO_T (15.05 wt%) which lends significant weight to the role of small polarons on conduction, in particular at lower crustal temperatures.

Dai et al. (2016) measure conductivity of an eclogite sample and observe a narrow range of ΔH values (0.79–0.86 eV) which are in good agreement with our higher temperature data, that is assuming our eclogite follows a similar trend to our granulite. Dai et al. (2016) attribute conduction within their eclogite to small polarons and attribute small discrepancies between their results and those of Bagdassarov et al. (2011) to mineralogical content, H_2O partitioning in omphacite, and slight differences in iron content in garnet. They do note that their results are in general agreement with those of Bagdassarov et al. (2011) after effects of pressure and fO_2 are both accounted for.

5.2.3. On anorthosites

Bai et al. (2002) measure conductivity of a slightly fluid-altered anorthosite consisting of plagioclase (70 wt%), zoisite (20 wt%) and sericite (10 wt%). Major compositional differences between their sample and ours are that their anorthosite has slightly elevated SiO_2 (54.86 wt%), and slightly lower FeO_T (1.12 wt%). Direct comparison shows that their results are similar to ours in terms of both activation energy and magnitude of conductivity (Fig. 7b). While the similarity is not unsurprising given that rocks of similar lithology should yield similar conductivity, we suggest that the marginally lower conductivity observed by Bai et al. (2002) is the result of slightly depleted Fe-content in their sample with comparison to ours and low concentration of impurities.

5.3. The effect of bulk composition

For granite samples measured at lower crustal conditions, Dai et al. (2014) use the geochemical index $X_A = (Na_2O + K_2O + CaO)/SiO_2$ to illustrate the effect of composition on conductivity. Their data show that an increase in X_A, from 0.10 to 0.16, can account for an increase of almost 1.5 orders of magnitude in conductivity at ~883 K. Despite this result, it is unclear if the relation holds true with reduced SiO_2 content as mafic rocks are generally enriched in Ca over Na, two elements that exhibit significantly different ΔH in plagioclase crystals (Yang et al., 2011a; Hu et al., 2013; Guo et al., 2015; Hu et al., 2015).

With more relevance to the lower crust, Sun et al. (2019) recently investigated the effect of composition for a set of three granulites with variable Fe content. In their experiment, they demonstrate enhanced conductivity up to one order of magnitude based on an increase in Fe content of ~9 wt%. Analysis of granulite compositions from the Global Geochemical Database (Gard et al., 2019) highlights significant variability in FeO_T with a standard deviation of 4.23 wt% around a mean of 8.24 wt% (Table 1; Fig. 8a). This distribution places their Fe-rich sample (14.79 wt%) just below the $+2$ standard deviation range and suggests that conductivity could vary by 1–1.5 orders of magnitude based on Fe content alone.

While such results are notable, the growing amount of experimental data on lower crustal rocks makes it possible to obtain more globally relevant information using a collective dataset. To do this, we reproduce experimental data using reported model parameters from references in Fig. 7b that also report geochemistry and are valid within the temperature range 773–973 K. We highlight the effect of FeO_T by plotting the collective dataset at a relatively moderate lower crustal temperature of 873 K (Fig. 8a). It is clear from Fig. 8a that conductivity is strongly dependent on FeO_T across the board; however, for mafic samples (≤ 55 wt% SiO_2) the relationship is strongly linear. A simple linear regression applied to data from mafic samples at 873 K (blue line; Fig. 8b) suggests that conductivity can realistically vary by up to 2.5 orders of magnitude based on FeO_T content alone. This effect is far stronger than that anticipated by Sun et al. (2019).

The linear relationship is unlikely to continue at low FeO_T concentrations ($< 1\sigma$ from the mean) as impurity conduction overtakes small polarons as the dominant mechanism. At the other end of the spectrum, FeO_T concentrations above one standard deviation — which statistically accounts for ~16% of granulites — may account for lower crustal conductivity up to ~300 Ω m at 873 K. At the upper limits of the compiled experimental data, 15 wt% FeO_T can account for conductivity in the lower crust up to 40 Ω m. Extrapolating to 20 wt%, provided the observed trend holds true, indicates that Fe-content may account for conductivity in the lower crust as high as 1 Ω m. To illustrate that the relationship holds true across a range of lower crustal temperatures, we also present the compiled mafic data on an Arrhenius plot with data coloured by FeO_T (Fig. 8b).

To increase the utility of our findings, we use multilinear regression to model conductivity as a function of both temperature and FeO_T within the temperature range 773–973 K. It can be seen in Fig. 8b that samples below ~5 wt% FeO_T are characterised by impurity conduction; therefore, these data are excluded from further modelling. Results from our regression analysis suggest that conductivity can be predicted to within 0.16 log units using

$$log\ \sigma(T, FeO_T) = 0.006 \pm 0.0002\ T + 0.3 \pm 0.004 FeO_T - 11.35 \pm 0.24, \quad (3)$$

where T is in kelvin and uncertainty is expressed as standard errors on the model coefficients. We suggest that deviations from this model for dry, mafic rocks are likely caused by sample impurities.

The model presented here has an advantage over mineral-based models due to a significant reduction in parameters. Whereby other models require estimates of temperature and modal proportions of plagioclase, pyroxene and garnet (plus any number of additional lower crustal minerals), our model requires only temperature and FeO_T. Mineral-based models also need to account for discrepancies between experiments that produce different results for the same mineral (e.g Romano et al., 2006; Dai et al., 2012) and need to account for the effect of solid-solutions (e.g. plagioclase; see Fig. 7a).

Because of the simplicity of our model, we are able to rearrange parameters in order to predict useful information from known conductivity. For instance, we remodel our synthetic dataset to establish the relationship

$$FeO_T (T, \sigma) = 37 \pm 0.83 - 0.0193 \pm 0.001\ T + 3.24 \pm 0.05\ log\ \sigma, \quad (4)$$

which allows us to estimate FeO_T of dry, mafic rocks at lower crustal temperatures to within ± 0.51 wt%. Alternatively, we can solve for T as a function of FeO_T and conductivity using
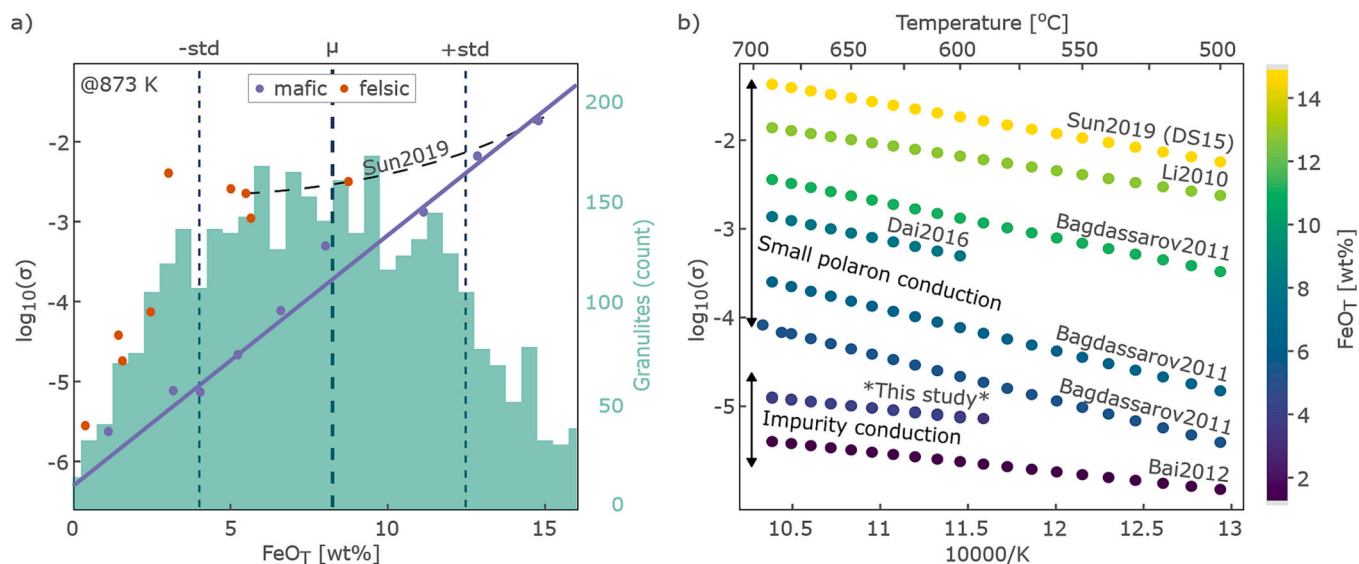
Fig. 8. The effect of FeO_T and temperature on electrical conductivity. a) conductivity of mafic (≤55 wt% SiO_2) and felsic (>55 wt% SiO_2) crustal rocks as a function of FeO_T at 873 K. Modelled fit to mafic data with $FeO_T > \mu - 1std$ (solid blue line; R^2 0.99) compared to trend identified by Sun et al. (2019). Below this cut-off, samples are dominated by impurity conduction. Histogram produced using 3649 granulite samples from the Global Geochemical Database (Gard et al., 2019). b) The relationship between conductivity, temperature and FeO_T for mafic, lower crustal rocks. Note: samples from this study plot almost directly on top of one another. (For interpretation of the references to colour in this figure legend, the reader is referred to the web version of this article.)

$$T(FeO_T, \sigma) = 1728 \pm 37.8 - 42 \pm 1.9 FeO_T + 139 \pm 6.1 \log \sigma, \quad (5)$$

in order to predict temperature to within 24 K. Obviously, uncertainties reported for Eqs. 4 and 5 are further compounded by inherent uncertainty in the resistivity models produced via the magnetotelluric method. However, such relationships will undoubtedly prove useful to researchers investigating the composition and thermal nature of the lower crust.

To briefly summarise, we use our newly established predictive models to determine the equivalent effect of increasing FeO_T versus increasing temperature on electrical conductivity. Using Eq. 3 to predict conductivity over the temperature range 773–973 K at an FeO_T of 8.24 wt% returns a conductivity range of $10^{-4.24}$ to $10^{-3.04}$ (or 0.6 log units per 100 K). Using this conductivity range in Eq. 4 at a temperature of 873 K returns an estimated FeO_T range of 6.41–10.3 wt% (or 0.31 log units per wt% FeO_T). These results suggest that an increase in FeO_T content of 2 wt% is roughly equivalent to increasing temperature in the lower crust by 100 K.

5.4. Model limitations

The findings described in the previous section regarding the relationship between FeO_T and electrical conductivity are significant but the models produced to describe that relationship are subject to certain limitations worth considering. To begin, the models are applied only to samples with <55 wt% SiO_2 and are therefore only relevant to a broadly mafic lower crust. While the assumption of a mafic lower crust is more generally confirmed by elevated seismic wave speeds and chemical analyses on xenoliths and granulite-facies terranes (Rudnick and Gao, 2014; Huang et al., 2013), Hacker et al. (2015) showed that wave speed data can, under certain conditions, be made to fit a felsic lower crust.

Any model produced using chemical composition alone neglects the effects of both mineralogy and geometric arrangement of constituent minerals. The specific minerals present in a rock will control important parameters for diffusion such as anion porosity which, in essence, dictates the free space available in a crystal lattice and therefore affects mobility of the charge carrier (Dowty, 1980). Additionally, the geometric arrangement of minerals in the rock will determine the specific mixing relationships required in order to determine bulk conductivity

(e.g. Selway, 2018; Ozaydın and Selway, 2020). Interconnectedness is also a requirement for current to flow and is a factor of both mineral proportions and geometric arrangement.

5.5. The effect of in-situ metasomatism

The effect of in-situ eclogitisation on electrical conductivity of the lower crust is likely to be variable and highly dependent on the bulk composition of the protolith. Results presented here suggest that fluid-catalysed conversion of dry lower crust does not significantly alter electrical conductivity, however, we stress that our samples contain very little iron, which is likely to be the main reactant with infiltrating fluids that can enhance conductivity. Fluids in the lower crust will always react with the host rock to form hydrous mineral assemblages (Yardley and Valley, 1997) and it is often thought that hydrous minerals will enhance conductivity thanks to the abundance of water. While free fluids can certainly exhibit this effect, hydroxyls bound to the crystal structure of a hydrous mineral require a larger degree of energy in order to move and produce an electric current.

Wang et al. (2012) measured the electrical conductivity of amphibole and determine that enhanced conductivity at temperatures >873 K is the result of dehydration related fluids that oxidise iron, thereby increasing the ratio of Fe^{3+} to Fe^{2+}, rather than conductive properties of the fluid itself. Logically, such a conclusion means that a rock with greater Fe content will see a far larger effect on conductivity in the presence of oxidising fluids than a comparable rock with lesser Fe content. For this reason, we conclude that, despite our samples indicating no effect of fluid alteration on electrical conductivity, such an effect is likely appreciable in rocks with greater Fe content. As our samples tend towards the low end of possible Fe concentrations for lower crustal rocks, we believe it possible that in-situ eclogitisation of the lower crust may indeed account for enhanced conductivity in regions characterised by more typical lower crustal compositions. Therefore, conductive anomalies in the lower crust may be the present-day observable signature of ancient subduction zones but further research is required to confirm this.

6. Conclusions

In-situ fluid-catalysed eclogitisation of dry, Fe-poor mafic granulite has no appreciable effect on electrical conductivity over reasonable lower crustal temperatures. Both samples measured in this study are extremely resistive due primarily to a relative lack of Fe and other charged species available for diffusion. At temperatures below 1000 K, the dominant mechanism is impurity conduction as evidenced by comparisons with experimental data from similar experiments on lower crustal rock types.

Above 1000 K, ascertaining the conduction mechanism is more complicated due to mineralogical heterogeneity and complex compositional relationships within mineral solid-solutions. In the end, we conclude that small polarons are the dominant conduction mechanism at higher temperatures in the granulite sample due to similarities with studies on garnet and clinopyroxene and a small but positive relationship between conductivity and increasing fO_2. Given the compositional similarity of both samples in this study, we assume the eclogite would replicate this change in dominant mechanism, however, experimental limitations, e.g. potential melting, prevented us from testing this assumption.

Our experimental observations indicate that highly conductive regions in the lower crust, as observed by many MT studies, cannot be explained by contiguous eclogite and granulite-facies terranes; however, variations in bulk composition between regions may produce vastly different outcomes. Further experimentation on Fe-rich, eclogitised lower crust and a known anhydrous protolith is required to fully answer this question.

A compilation of previous experimental data on a range of relevant mafic to felsic rock types indicates a strong relationship between electrical conductivity and bulk composition. For dry, mafic lower crustal rocks (SiO_2 < 55 wt%), a strong linear relationship exists between conductivity and FeO_T over the temperature range 773 to 973 K. Modelling this relationship suggests that reasonable variations in FeO_T (4–12.5 wt%) over lower crustal temperatures (773–973 K) can account for variable resistivity in the lower crust up to 3.7 orders of magnitude. Within this range, maximum conductivity of ~60 Ω m occurs at 973 K and 12.5 wt% FeO_T while maximum resistivity of $10^{5.5}$ Ω m occurs at 773 K and 4 wt% FeO_T.

Abnormally high (but not unreasonable) FeO_T concentrations up to 20 wt% can account for conductive anomalies in the lower crust up to ~1 Ω m at a relatively moderate 873 K.

We establish a system of linear equations that may be used to estimate conductivity, Fe-content or temperature within dry, mafic lower crust. Conductivity may be estimated within the temperature range 773–973 K to within 0.16 log units using $\log \sigma(T,FeO_T) = 0.006\,T + 0.3FeO_T - 11.35$. FeO_T () may be estimated within the same temperature range to within 0.51 wt% using $FeO_T(T,\sigma) = 37 - 0.0193\,T + 3.24\log \sigma$. Finally, using conductivity and an estimate of FeO_T, it is possible to estimate temperature to within 31 K using $T(FeO_T,\sigma) = 1728 - 42FeO_T + 139\log \sigma$. With regards to conductivity in dry, mafic lower crust, these relationships suggest that an increase in FeO_T of 2 wt% is roughly equivalent to increasing temperature by 100 K.

CRediT authorship contribution statement

S. Jennings: Methodology, Software, Validation, Formal analysis, Investigation, Writing – original draft, Visualization. **D. Hasterok:** Project administration, Conceptualization, Methodology, Resources, Funding acquisition, Writing – review & editing, Supervision. **M. Hand:** Project administration, Funding acquisition, Writing – review & editing, Supervision, Investigation. **K. Bhowany:** Formal analysis, Investigation, Writing – review & editing.

Declaration of Competing Interest

The authors declare that they have no known competing financial interests or personal relationships that could have appeared to influence the work reported in this paper.

Data availability

Data will be made available on request.

References

Andersen, T., Austrheim, H., Burke, E.A.J., Elvevold, S., 1993. N2 and CO2 in deep crustal fluids: evidence from the Caledonides of Norway. Chem. Geol. 108, 113–132. URL: http://www.sciencedirect.com/science/article/pii/000925419390320I, doi: 10.1016/0009-2541(93) 90320-I. fluid-rock Interaction in the Deeper Continental Lithosphere.

Austrheim, H., 2013. Fluid and deformation induced metamorphic processes around Moho beneath continent collision zones: examples from the exposed root zone of the Caledonian mountain belt, W-Norway. Tectonophysics 609, 620–635. https://doi.org/10.1016/j.tecto.2013.08.030.

Bagdassarov, N., Batalev, V., Egorova, V., 2011. State of lithosphere beneath Tien Shan from petrology and electrical conductivity of xenoliths. J. Geophys. Res. Solid Earth 116. https://doi.org/10.1029/2009JB007125.

Bai, L.P., Du, J.G., Liu, W., Zhou, W.G., 2002. The experimental studies on electrical conductivities and P-wave velocities of anorthosite at high pressure and high temperature. Acta Seismol. Sin. 15, 667–676. https://doi.org/10.1007/s11589-002-0091-1.

Bhowany, K., Hand, M., Clark, C., Kelsey, D.E., Reddy, S.M., Pearce, M.A., Tucker, N.M., Morrissey, L.J., 2017. Phase equilibria modelling constraints on P-T conditions during fluid catalysed conversion of granulite to eclogite in the Bergen Arcs, Norway. J. Metamorph. Geol. 36, 315–342. https://doi.org/10.1111/jmg.12294.

Bose, S., Das, K., Ohnishi, I., Torimoto, J., Karmakar, S., Shinoda, K., Dasgupta, S., 2009. Characterization of oxide assemblages of a suite of granulites from Eastern Ghats Belt, India: Implication to the evolution of C–O–H–F fluids during retrogression. Lithos 113, 483–497. URL: http:// www.sciencedirect.com/science/article/pii/S0024493709002412. https://doi.org/10.1016/j.lithos.2009.05.029.

Chakraborty, S., 2008. Diffusion in solid silicates: a tool to track timescales of processes comes of age. Annu. Rev. Earth Planet. Sci. 36, 153–190. https://doi.org/10.1146/annurev.earth.36. 031207.124125.

Dai, L., Li, H., Hu, H., Shan, S., Jiang, J., Hui, K., 2012. The effect of chemical composition and oxygen fugacity on the electrical conductivity of dry and hydrous garnet at high temperatures and pressures. Contrib. Mineral. Petrol. 163, 689–700. https://doi.org/10.1007/s00410-011-0693-5.

Dai, L., Hu, H., Li, H., Jiang, J., Hui, K., 2014. Influence of temperature, pressure, and chemical composition on the electrical conductivity of granite. Am. Mineral. 99, 1420–1428. https://doi.org/10.2138/am.2014.4692.

Dai, L., Hu, H., Li, H., Wu, L., Hui, K., Jiang, J., Sun, W., 2016. Influence of temperature, pressure, and oxygen fugacity on the electrical conductivity of dry eclogite, and geophysical implications. Geochem. Geophys. Geosyst. 17, 2394–2407. https://doi.org/10.1002/2016GC006282.

Dai, L., Sun, W., Li, H., Hu, H., Wu, L., Jiang, J., 2018. Effect of chemical composition on the electrical conductivity of gneiss at high temperatures and pressures. Solid Earth 9, 233–245. URL: https ://se.copernicus.org/articles/9/233/2018/. https://doi.org/10.5194/se-9-233-2018.

Dowty, E., 1980. Crystal-chemical factors affecting the mobility of ions in minerals. Am. Mineral. 65, 174–182. URL: https://pubs.geoscienceworld.org/msa/ammin/article/65/1-2/174/41110.

Fuji-ta, K., Katsura, T., Tainosho, Y., 2004. Electrical conductivity measurement of granulite under mid- to lower crustal pressure—temperature conditions. Geophys. J. Int. 157, 79–86. https://doi.org/10.1111/j.1365-246X.2004.02165.x.

Gard, M., Hasterok, D., Halpin, J.A., 2019. Global whole-rock geochemical database compilation. Earth Syst. Sci. Data 11, 1553–1566. https://doi.org/10.5194/essd-11-1553-2019.

Guo, Y., Wang, D., Shi, Y., Zhou, Y., Dong, Y., Li, C., 2014. The electrical conductivity of eclogite in Tibet and its geophysical implications. Sci. China Earth Sci. 57, 2071–2078. https://doi.org/10.1007/s11430-014-4876-6.

Guo, X., Yoshino, T., Shimojuku, A., 2015. Electrical conductivity of albite–(quartz)–water and albite– water–NaCl systems and its implication to the high conductivity

anomalies in the continental crust. Earth Planet. Sci. Lett. 412, 1–9. URL: https://www.sciencedirect.com/science/article/pii/S0012821X14007821.

Hacker, B.R., Kelemen, P.B., Behn, M.D., 2015. Continental lower crust. Annu. Rev. Earth Planet. Sci. 43, 167–205. https://doi.org/10.1146/annurev-earth-050212-124117.

Harlov, D.E., 2000. Titaniferous magnetite–ilmenite thermometry and titaniferous magnetite–ilmenite– orthopyroxene–quartz oxygen barometry in granulite facies gneisses, Bamble Sector, SE Norway: implications for the role of high-grade CO2-rich fluids during granulite genesis. Contrib. Mineral. Petrol. 139, 180–197.

Hu, H., Li, H., Dai, L., Shan, S., Zhu, C., 2013. Electrical conductivity of alkali feldspar solid solutions at high temperatures and high pressures. Phys. Chem. Miner. 40, 51–62.

Hu, H., Dai, L., Li, H., Jiang, J., Hui, K., 2014. Electrical conductivity of K-feldspar at high temperature and high pressure. Mineral. Petrol. 108, 609–618.

Hu, H., Dai, L., Li, H., Hui, K., Li, J., 2015. Temperature and pressure dependence of electrical conductivity in synthetic anorthite. Solid State Ionics 276, 136–141. URL: https://www.sciencedirect.com/science/article/pii/S0167273815001551. https://doi.org/10.1016/j.ssi.2015.04.008.

Hu, H., Dai, L., Sun, W., Wang, M., Jing, C., 2022. Constraints on fluids in the continental crust from laboratory-based electrical conductivity measurements of plagioclase. Gondwana Res. 107, 1–12. https://doi.org/10.1016/j.gr.2022.02.011.

Huang, Y., Chubakov, V., Mantovani, F., Rudnick, R.L., McDonough, W.F., 2013. A reference earth model for the heat-producing elements and associated geoneutrino flux, heat flow. Geochem. Geophys. Geosyst. 14, 2003–2029. https://doi.org/10.1002/ggge.20129.

Karato, S.I., Dai, L., 2009. Comments on "Electrical conductivity of wadsleyite as a function of temperature and water content" by Manthilake et al. Phys. Earth Planet. Inter. 174, 19–21. URL: https://www.sciencedirect.com/science/article/pii/S0031920109000120. https://doi.org/10.1016/j.pepi.2009.01.011 (advances in High Pressure Mineral Physics: from Deep Mantle to the Core).

Katayama, I., Nakashima, S., Yurimoto, H., 2006. Water content in natural eclogite and implication for water transport into the deep upper mantle. Lithos 86, 245–259. URL: https://www.sciencedirect. com/science/article/pii/S0024493705001490. https://doi.org/10.1016/j.lithos.2005.06.006.

Laštovičková, M., Parchomenko, E.I., 1976. The electric properties of eclogites from the bohemian massif under high temperatures and pressures. Pure Appl. Geophys. 114, 451–460. https://doi.org/10.1007/BF00876944.

Li, P., Zhou, W.G., Gong, C.Y., Fan, D.W., Wei, S.Y., Xie, H.S., 2010. Electrical conductivity of twopyroxene granulite under high pressure in northern margin of North China craton. Chin. J. Geophys. 53, 794–804. https://doi.org/10.1002/cjg2.1549.

Liu, H., Zhu, Q., Yang, X., 2019. Electrical conductivity of OH-bearing omphacite and garnet in eclogite: the quantitative dependence on water content. Contrib. Mineral. Petrol. 174, 57. https://doi.org/10.1007/s00410-019-1593-3.

Manthilake, G., Bolfan-Casanova, N., Novella, D., Mookherjee, M., Andrault, D., 2016. Dehydration of chlorite explains anomalously high electrical conductivity in the mantle wedges. Sci. Adv. 2, e1501631 https://doi.org/10.1126/sciadv.1501631.

McCammon, C., 2005. GEOCHEMISTRY: the paradox of mantle redox. Science 308, 807–808. https://doi.org/10.1126/science.1110532.

Medaris, L.G., Beard, B.L., Johnson, C.M., Valley, J.W., Spicuzza, M.J., Jelínek, E., Misar, Z., 1995. Garnet pyroxenite and eclogite in the bohemian massif: geochemical evidence for Variscan recycling of subducted lithosphere. Geol. Rundsch. 84, 489–505. https://doi.org/10.1007/BF00284516.

Ozaydın, S., Selway, K., 2020. MATE: an analysis tool for the interpretation of magnetotelluric models of the mantle. Geochem. Geophys. Geosyst 21 https://doi.org/10.1029/2020GC009126.

Romano, C., Poe, B.T., Kreidie, N., McCammon, C.A., 2006. Electrical conductivities of pyropealmandine garnets up to 19 GPa and 1700 °C. Am. Mineral. 91, 1371–1377. https://doi.org/10.2138/am.2006.1983.

Rudnick, R.L., Gao, S., 2014. Composition of the continental crust. In: Treatise on Geochemistry, , 2nd edvol. 4. Elsevier-Pergamon, Oxford, UK, pp. 1–51. The Crust.

Selway, K., 2014. On the causes of electrical conductivity anomalies in tectonically stable lithosphere. Surv. Geophys. 35, 219–257. https://doi.org/10.1007/s10712-013-9235-1.

Selway, K., 2018. Electrical discontinuities in the continental lithosphere imaged with magnetotellurics. Lithospheric Discontinuities 89–109.

Shankland, T.J., Ander, M.E., 1983. Electrical conductivity, temperatures, and fluids in the lower crust. J. Geophys. Res. Solid Earth 88, 9475–9484. https://doi.org/10.1029/JB088iB11p09475.

Sun, W., Dai, L., Li, H., Hu, H., Jiang, J., Hui, K., 2017. Effect of dehydration on the electrical conductivity of phyllite at high temperatures and pressures. Mineral. Petrol. 111, 853–863. https://doi.org/10.1007/s00710-017-0494-2.

Sun, W., Dai, L., Li, H., Hu, H., Liu, C., 2019. Effect of temperature, pressure and chemical composition on the electrical conductivity of granulite and geophysical implications. J. Mineral. Petrol. Sci. 181107b. https://doi.org/10.2465/jmps.181107b.

Tamblyn, R., Brown, D., Hand, M., Morrissey, L., Clark, C., Anczkiewicz, R., 2020. The 2 Ga eclogites of Central Tanzania: directly linking age and metamorphism. Lithos 105890. https://doi.org/10.1016/j.lithos. 2020.105890.

Tyburczy, J.A., Roberts, J.J., 1990. Low frequency electrical response of polycrystalline olivine compacts: grain boundary transport. Geophys. Res. Lett. 17, 1985–1988. https://doi.org/10.1029/GL017i011p01985.

Wang, D., Guo, Y., Yu, Y., Karato, S.I., 2012. Electrical conductivity of amphibole-bearing rocks: influence of dehydration. Contrib. Mineral. Petrol. 164, 17–25.

Wannamaker, P.E., Caldwell, T.G., Jiracek, G.R., Maris, V., Hill, G.J., Ogawa, Y., Bibby, H.M., Bennie, S.L., Heise, W., 2009. Fluid and deformation regime of an advancing subduction system at Marlborough, New Zealand. Nature 460, 733–736. https://doi.org/10.1038/nature08204.

Wright, A.E., 1990. Granulite. Springer US, Boston, MA, pp. 204–205. https://doi.org/10.1007/0-387-30845-8_85.

Yang, X., 2011. Origin of high electrical conductivity in the lower continental crust: a review. Surv. Geophys. 32, 875–903. https://doi.org/10.1007/s10712-011-9145-z.

Yang, X., Keppler, H., McCammon, C., Ni, H., 2011a. Electrical conductivity of orthopyroxene and plagioclase in the lower crust. Contrib. Mineral. Petrol. 163, 33–48. https://doi.org/10.1007/s00410-011-0657-9.

Yang, X., Keppler, H., McCammon, C., Ni, H., Xia, Q., Fan, Q., 2011b. Effect of water on the electrical conductivity of lower crustal clinopyroxene. J. Geophys. Res. 116 https://doi.org/10.1029/2010jb008010.

Yardley, B.W.D., Valley, J.W., 1997. The petrologic case for a dry lower crust. J. Geophys. Res. Solid Earth 102, 12173–12185. https://doi.org/10.1029/97JB00508.

Yoshino, T., Nishi, M., Matsuzaki, T., Yamazaki, D., Katsura, T., 2008. Electrical conductivity of majorite garnet and its implications for electrical structure in the mantle transition zone. Phys. Earth Planet. Inter. 170, 193–200. https://doi.org/10.1016/j.pepi.2008.04.009.

Zhang, B., Yoshino, T., 2016. Effect of temperature, pressure and iron content on the electrical conductivity of orthopyroxene. Contrib. Mineral. Petrol. 171, 102. https://doi.org/10.1007/s00410-016-1315-z.